

## Using scaling relations to understand trends in the catalytic activity of transition metals

This article has been downloaded from IOPscience. Please scroll down to see the full text article.

2008 J. Phys.: Condens. Matter 20 064239

(<http://iopscience.iop.org/0953-8984/20/6/064239>)

View [the table of contents for this issue](#), or go to the [journal homepage](#) for more

Download details:

IP Address: 129.252.86.83

The article was downloaded on 29/05/2010 at 10:33

Please note that [terms and conditions apply](#).

# Using scaling relations to understand trends in the catalytic activity of transition metals

G Jones<sup>1</sup>, T Bligaard<sup>1</sup>, F Abild-Pedersen<sup>1,2</sup> and J K Nørskov<sup>1,3</sup>

<sup>1</sup> Center for Atomic-scale Materials Design, Department of Physics, NanoDTU, Technical University of Denmark, DK-2800 Lyngby, Denmark

<sup>2</sup> Computational Materials Design ApS, Building 307, DTU, DK-2800 Lyngby, Denmark

E-mail: [norskov@fysik.dtu.dk](mailto:norskov@fysik.dtu.dk)

Received 9 November 2007, in final form 29 November 2007

Published 24 January 2008

Online at [stacks.iop.org/JPhysCM/20/064239](http://stacks.iop.org/JPhysCM/20/064239)

## Abstract

A method is developed to estimate the potential energy diagram for a full catalytic reaction for a range of late transition metals on the basis of a calculation (or an experimental determination) for a single metal. The method, which employs scaling relations between adsorption energies, is illustrated by calculating the potential energy diagram for the methanation reaction and ammonia synthesis for 11 different metals on the basis of results calculated for Ru. It is also shown that considering the free energy diagram for the reactions, under typical industrial conditions, provides additional insight into reactivity trends.

## 1. Introduction

Computational methods based on density functional theory (DFT) have attained sufficient accuracy and efficiency that they can be used to describe surface chemical processes of interest in heterogeneous catalysis. There are a number of cases where complete catalytic reactions on surfaces have been outlined in terms of activation energies and reaction energies [1–8] and considerable insight has been obtained about mechanisms and kinetics in this way. Such calculations are, however, quite demanding. While there are examples where a family of catalysts have been investigated in this way [9], extensive calculations of whole reaction pathways are typically done for a single metal and a single surface.

In the present paper we introduce a method for evaluating reaction energies for all steps in a catalytic reaction on a range of transition metal surfaces on the basis of a database of adsorption energies of a few atoms and molecules—C, O, H, N, and CO. The key to the new method is the recent discovery of scaling relations between the adsorption energies of different partially hydrogenated intermediates [10]. We will show that it is possible to quite easily generate data for a number of metals and in this way obtain reactivity trends. We also show that the reaction energies can be used to generate families of free energy diagrams for complete reactions. The approach

is illustrated by applying it to two simple catalytic reactions, the methanation reaction and the ammonia synthesis reaction. We use it to show how an overview of reactivity trends can be generated.

## 2. Methodology

All of the presented results are calculated using self-consistent DFT. Ionic cores and their interaction with valence electrons are described by ultra-soft pseudopotentials and the valence wavefunctions are expanded in a basis set of plane waves with a kinetic energy cut-off of 340 eV. Exchange and correlation effects are taken into account through the RPBE [11] generalized gradient approximation (GGA). The electron density of the valence states is obtained by a self-consistent iterative diagonalization of the Kohn–Sham Hamiltonian with Pulay mixing of the densities. The occupation of the one-electron states is calculated using a temperature of  $k_B T = 0.1$  eV; all energies are extrapolated to  $T = 0$  K. The ionic degrees of freedom are relaxed using the quasi-Newton minimization scheme, until the maximum force component is found to be smaller than  $0.05$  eV  $\text{\AA}^{-1}$ . Spin magnetic moments for Fe, Co and Ni are taken into account.

We use the periodic slab approximation and the considered unit cells are chosen so that an equivalent of three layers in the most close-packed direction is obtained. Neighboring slabs

<sup>3</sup> Author to whom any correspondence should be addressed.

are separated by more than 10 Å of vacuum. The adsorbate together with the topmost close-packed layer of the unit cell is allowed to relax fully. The Brillouin zone of the systems is sampled with a  $4 \times 4 \times 1$  Monkhorst–Pack grid.

### 3. Scaling relations, potential energy and free energy diagrams

By performing DFT calculations for a large number of adsorbates and transition metal surfaces it has been discovered that the adsorption energy for molecules of the type  $AH_x$  is linearly correlated with the adsorption energy of atom A:

$$\Delta E^{AH_x} = \gamma(x) \Delta E^A + \xi \quad (1)$$

Figure 1 shows these scaling relations holding for a large number of (late) transition metals. It also shows that the scaling parameters only depend on the molecule in question and are given to a good approximation by

$$\gamma(x) = (x_{\max} - x)/x_{\max}, \quad (2)$$

where  $x_{\max}$  is the maximum number of H atoms that can bond to the central atom A ( $x_{\max} = 4$  for A = C,  $x_{\max} = 3$  for A = N, and  $x_{\max} = 2$  for A = O), i.e. the number of hydrogen atoms that the central atom, A, would bond to in order to form neutral gas-phase molecules according to the octet rule.

The scaling relations, however, cannot be understood simply in terms of bond counting. C bonded to the three-fold site on an fcc(111) surface does not bond to four metal atoms, for instance, and the scaling relations are independent of the adsorption site. If the C atoms are moved to a one-fold site approximately the same slope appears in a plot like figures 1(a)–(c) (the  $x$ -axis is simply shifted by the difference in C adsorption energy on the three- and one-fold sites). Rather, the scaling behavior can be viewed as an illustration of bond order conservation [10].

There is some scatter in the data in figure 1, corresponding to a mean absolute error of 0.1–0.2 eV depending on the intermediate and the surface structure. A large part of this error stems from the fact that adsorption sites change as the number of H atoms in the molecule changes.  $CH_3$ , for instance, typically adsorbs in a one-fold site on close-packed transition metal surfaces while C adsorbs in three-fold sites. If one uses C adsorption energies calculated for one-fold adsorption geometries in figure 1(c), the mean absolute error is halved [10].

The scaling relations can be used directly to obtain reaction energies for a full catalytic reaction in the following way. We first consider reactions that only involve hydrogen-containing intermediates of the type  $AH_x$  with A = C, N or O. If we have calculated the energy of all reaction intermediates,  $\Delta E_{M1}^{AH_x}$ , for one metal, M1, we can estimate the energy,  $\Delta E_{M2}^{AH_x}$ , of the same intermediate on another metal, M2, from the adsorption energies of atom A on the two metals as:

$$\Delta E_{M2}^{AH_x} = \Delta E_{M1}^{AH_x} + \gamma(x) (\Delta E_{M2}^A - \Delta E_{M1}^A), \quad (3)$$

where  $\gamma(x)$  is a rational number given by equation (2). If we have a database of atomic adsorption energies for a number of metals we can therefore estimate all reaction intermediates.

It turns out that this approach is reasonable also if one tries to estimate bond energies for sigma-type bonds between more complicated molecules and the late transition metals. For such systems equation (3) is still expected to be approximately valid for each atom, A, making a bond to the surface, provided the definition of  $\gamma(x)$  is generalized to include contributions from all intra-molecular covalent bonds that atom A participates in:

$$\gamma(x, x_{\text{intra}}) = (x_{\max} - x - x_{\text{intra}})/x_{\max}. \quad (4)$$

The introduction of intra-molecular bonds may result in interactions between adsorbate pi-states and the metal-states. This leads to complications and one need to consider the reactivity of the metal in question and its ability to break any pi-bonds that are present. If we take as an example an ethylene molecule binding to a late transition metal surface that is able to break the molecular pi-bond, thus making two sigma-bonds to the surface, the  $\gamma(x)$  to be used in equation (3) will be  $\gamma(2, 1) = (4 - 2 - 1)/4 = 1/4$  for each of the two C atoms. A detailed analysis of this is the subject of a forthcoming publication.

In the following we will use equation (3) to construct approximate potential energy diagrams for a range of transition metals based on a calculation for a single metal. In addition to potential energy diagrams, we will also be interested in free energy diagrams. Free energies for gas-phase species are calculated by employing standard formulae for the statistical thermodynamics of a classical ideal gas [12]. For the gas-phase species ( $X$ ) at temperature ( $T$ ) and pressure ( $P$ ), the Gibbs free energy ( $G_X^{P,T}$ ) is given by:

$$G_X^{P,T} = E_X + E_{ZPE} + \Delta H^{0,T} - TS^T + RT \ln(P/P^o), \quad (5)$$

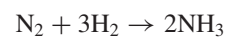
where  $E_X$  is the energy of  $X$ ,  $E_{ZPE}$  is the zero point energy,  $\Delta H^{0,T}$  is the enthalpy change in going from a temperature of 0 K to the temperature  $T$ ,  $S^T$  is the entropy at  $T$ ,  $R$  is the universal gas constant and  $P^o$  is standard pressure (taken to be 1 bar). The equation for the adsorbed species ( $X'$ ) on metal (M) is similar;  $E_{X'}$  is given by  $E_{MX'} - E_M$ , there is no pressure term and the enthalpy change is replaced by the change in internal energy. This leads to the following expression for ( $G_{X'}^{P,T}$ ):

$$G_{X'}^{P,T} = E_{X'} + E_{ZPE} + \Delta U^{0,T} - TS^T. \quad (6)$$

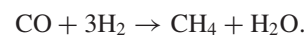
All vibrational frequencies used to determine  $E_{ZPE}$ ,  $\Delta U^{0,T}$  and  $S^T$  are calculated within the harmonic approximation.

### 4. Application to two reactions

The two reactions we consider in the following are the ammonia synthesis reaction



and the methanation reaction



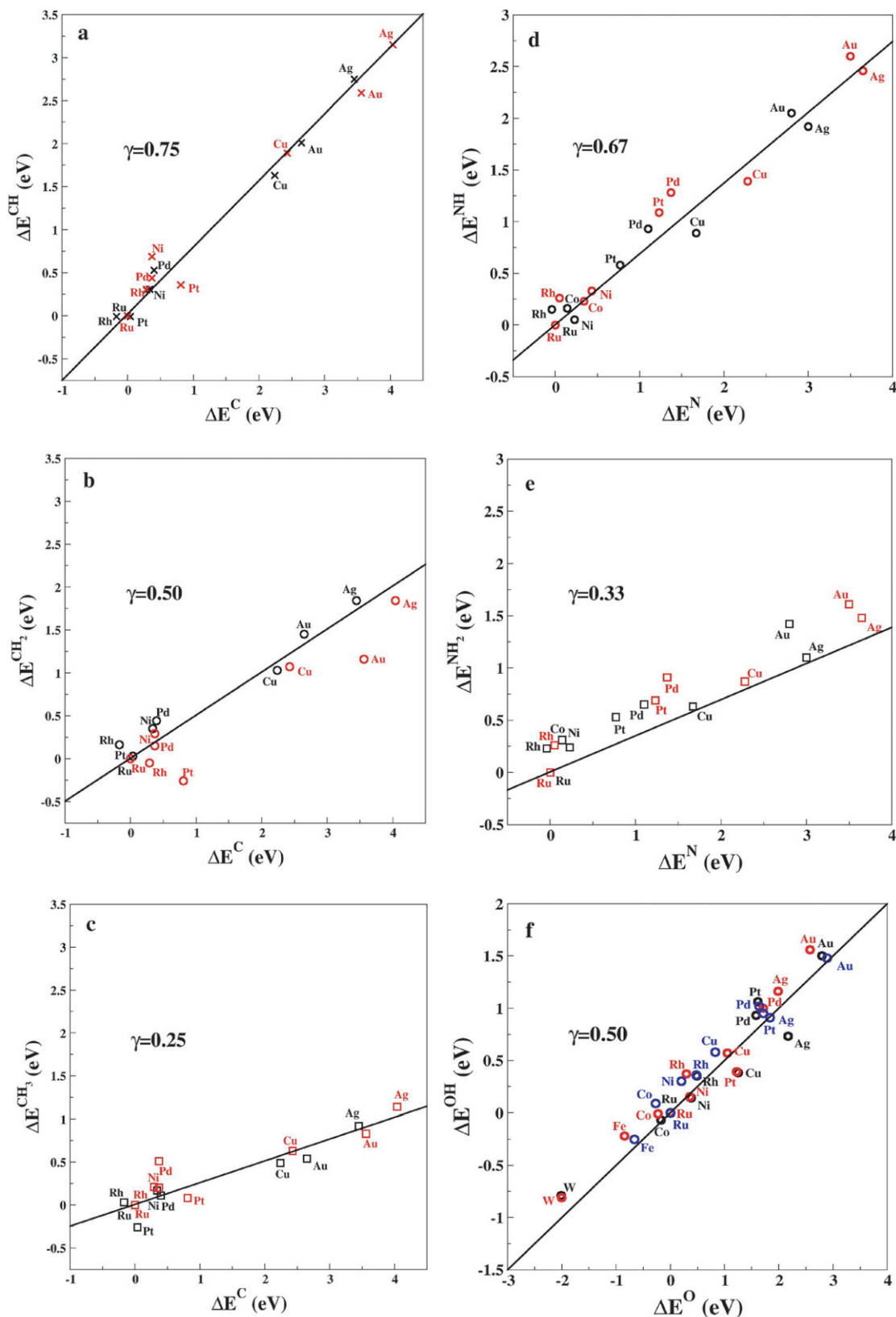


**Figure 1.** (a)–(c) Calculated adsorption energies of  $CH_x$  intermediates, (d) and (e)  $NH_x$  intermediates and (f) OH intermediates shown as a function of the adsorption energies of atomic C, N and O, respectively. The adsorption energy of molecule A on a given metal M is defined relative to the adsorption of A on  $M = Ru$ . The data presented have been taken from [10]. A line through (0, 0) with the theoretically predicted slope is drawn in each plot to indicate the accuracy of the results presented in this paper. Red points corresponds to adsorption on fcc(211) steps, black points correspond to the fcc(111) terrace, and the blue points correspond to adsorption on fcc(100) surfaces.

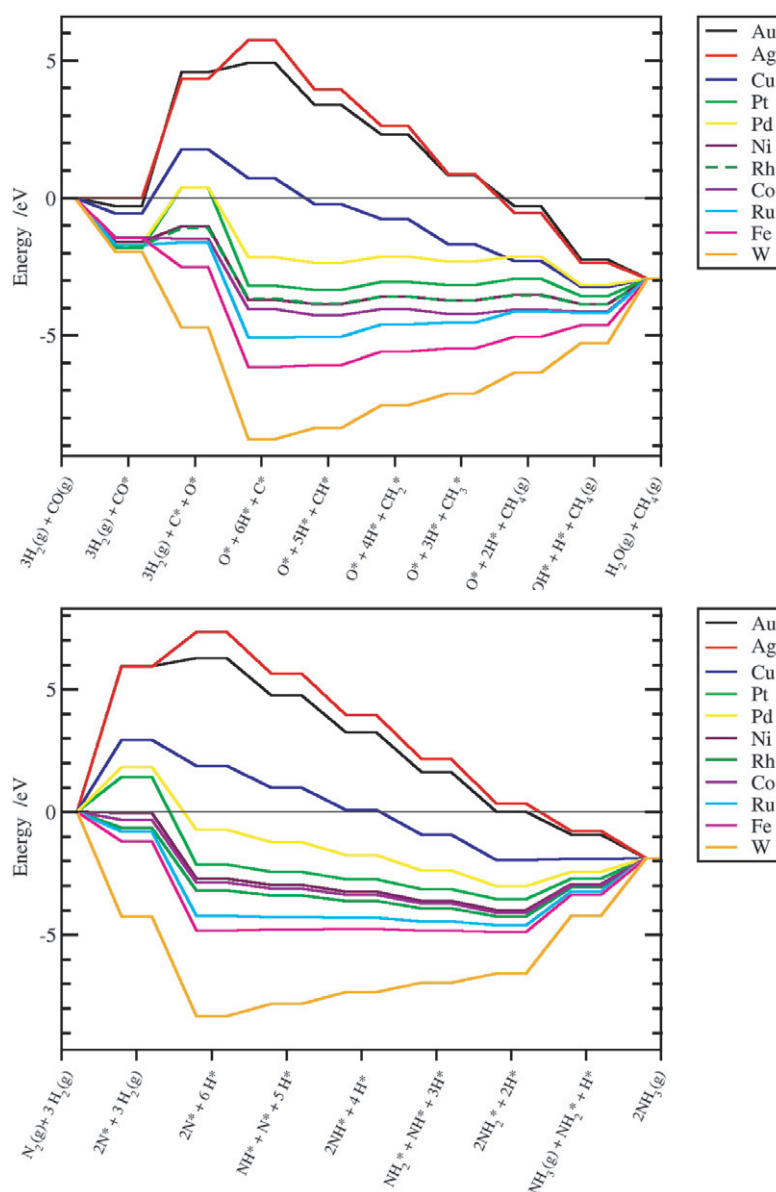


**Figure 2.** Potential energy diagrams showing the energy of all intermediates in the methanation and ammonia synthesis reactions. The result for Ru is from a full density functional theory calculation while the data for all other metals have been estimated using the scaling relations, equation (3).

They are two of the simplest reactions in heterogeneous catalysis and are very well studied, both experimentally [13–15] and theoretically [16, 17, 1]. They are therefore well suited for testing new methods.

For both reactions a complete DFT calculation has been done for Ru, while the results for other metals have been obtained using the scaling relations, equation (3), with the scaling constants given by equation (4). In both cases the calculations have been performed for stepped crystals, as they have been found theoretically to be the most active for both reactions [18]. The results for the ammonia synthesis have been taken from [19], while those for the methanation reaction are from the present study. The differences in adsorption energies of C, N and O on different metals have been taken from the DFT generated databases published in [16]. Here

we have also found adsorption energies of H and CO on the different metals.

Figure 2 shows the potential energy diagram for all intermediates for 11 different late transition metals. In constructing the potential energy diagram, we have assumed a particular reaction mechanism, the simplest one usually employed in describing these reactions. Other mechanisms could be possible, but for the present purpose of illustrating the capabilities of the method we employ only this one mechanism for each reaction.

It is evident from the potential energy diagrams that there is a substantial spread in the energies of the intermediates for the range of metals considered. From one metal to the next the stability of the intermediates typically differs by of the order 1 eV. This means first of all that the present analysis is quite

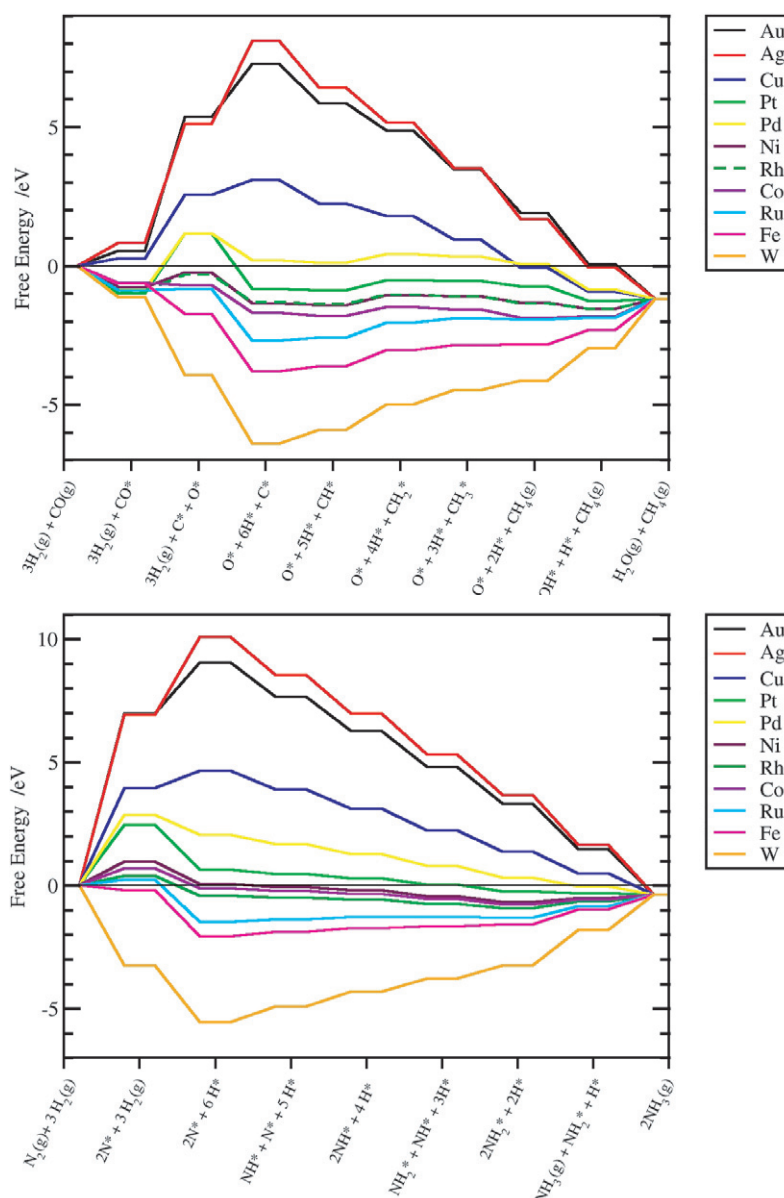


**Figure 3.** Free energy diagrams for the methanation and ammonia synthesis reactions for a number of metals. In both cases realistic industrial conditions and a stoichiometric reactant mixture has been used: Methanation: 30 bar, 475 K, 90% conversion. Ammonia synthesis: 100 bar, 675 K, 20% conversion.

meaningful. The mean average error expected in figure 2 must be of the same order of magnitude as that in figure 1, which is 0.1–0.2 eV. This is quite a small error when comparing the elemental metals.

The large spread also means that differences in catalytic activity between different metals are not due to subtleties. Ru and Ni, for instance, show differences in energies of intermediates of up to 1.5 eV, yet the catalytic rates under typical methanation conditions differ by less than an order of magnitude [16]. This shows that the rate of a complete catalytic reaction is quite a robust quantity, an observation that could be related to a compensation of different reaction steps [19, 20]. Often, if one reaction step becomes faster on going from one metal to the next, another will become slower (if adsorption becomes faster because stronger bonds can be

made to the surface, desorption becomes slower since it is now more difficult to break bonds again). A change in metal can therefore result in large changes in rates of elementary steps, but these changes may compensate each other to minimize the change in the overall rate.

In order to learn more about the reactivity of different metals under realistic reaction conditions it is useful not only to consider the potential energy diagram for a reaction but also the free energy diagram. The free energy diagrams in figure 3 have been generated in the following way: adsorbed molecular CO and atomic H have been assumed in equilibrium with the initial state, while all other intermediates have been assumed in equilibrium with the final state of the reaction. Typical industrial reaction conditions have been chosen for the two reactions. The configurational entropy of the adsorbed state



is not included and the values are therefore ‘standard’ free energies in the sense that they all refer to half a monolayer of adsorbate in each state. The free energy diagrams are the correct free energy diagrams for the two reactions if CO or N<sub>2</sub> dissociation is rate limiting (which is correct for a number of metals). This is just a convention, though, and the relative free energies from figure 3 can be used to tell whether there is a tendency to build up coverage of a certain intermediate on the surface. Given the free energy diagrams it is quite simple to understand qualitatively why certain metals are better suited than others as catalysts for the two reactions.

The best elemental methanation catalysts are known to be Co, Ru, Ni and Rh [16], and figure 3 illustrates why. Au, Ag, Cu, Pt and Pd all bind C and O too weakly to build up an appreciable coverage of these species on the surface, even if CO dissociation was fast. Since the activation barrier also depends strongly on the reaction energy for dissociation through Brønsted–Evans–Polanyi-type relationships [18, 21–23], a high free energy of the dissociation product is also an indication of a high dissociation barrier. Fe and W, on the other hand, bind C and O very strongly and are hence expected to build up a high coverage and eventually turn into oxides or carbides. The best catalysts are observed to be those where the intermediates have free energies following as closely as possible the interpolated free energy path between the initial and final states.

The picture is the same for the ammonia synthesis reaction. Of the metals considered here, Ru and Fe are known experimentally [24] and theoretically [25] to be the best catalysts followed by Rh. It is evident from figure 3 that these are indeed the metals that have the smallest maxima and minima linking the initial and final states. All the noble metals bind N atoms too weakly, while W binds them too strongly. Note that in general there is a shift towards weaker bonding for all the metals when the ammonia synthesis free energy diagrams are compared with those for the methanation reaction. This reflects the fact that the best ammonia synthesis catalysts tend to be a little less noble than the best methanation catalysts.

## 5. Conclusions

In the present paper we have established a simple way of estimating reaction free energies based on scaling relations between adsorption energies within DFT. We have shown that it is possible to get qualitative agreement between DFT and what is found experimentally for the methanation and ammonia synthesis reaction. With this knowledge we can then use a limited number of DFT calculations combined with the models developed based on these calculations to screen for new catalysts with a better catalytic performance.

## Acknowledgments

The Center for Atomic-scale Materials Design is funded by the Lundbeck Foundation. The authors wish to acknowledge additional support from the Danish Research Agency through grant 26-04-0047 and the Danish Center for Scientific Computing through grant HDW-0107-07.

## References

- [1] Alavi A, Hu P, Deutsch T, Silvestrelli P L and Hutter J 1998 *Phys. Rev. Lett.* **80** 3650
- [2] Eichler A and Hafner J 1999 *Phys. Rev. B* **59** 5960
- [3] Hammer B 2001 *J. Catal.* **199** 171
- [4] Logadottir A and Nørskov J K 2003 *J. Catal.* **220** 273
- [5] Linic S and Barteau M A 2003 *J. Am. Chem. Soc.* **125** 4034
- [6] Ovesson S, Lundqvist B I, Schneider W F and Bogicevic A 2005 *Phys. Rev. B* **71** 115406
- [7] Reuter K, Frenkel D and Scheffler M 2004 *Phys. Rev. Lett.* **93** 116105
- [8] Kandoi S, Greeley J, Sanchez-Castillo M A, Evans S T, Gokhale A A, Dumesic J A and Mavrikakis M 2006 *Top. Catal.* **37** 17
- [9] Falsig H, Bligaard T, Christensen C H and Nørskov J K 2007 *Pure Appl. Chem.* at press
- [10] Abild-Pedersen F, Greeley J, Studt F, Rossmeisl J, Munter T R, Moses P G, Skúlason E, Bligaard T and Nørskov J K 2007 *Phys. Rev. Lett.* **99** 016105
- [11] Hammer B, Hansen L B and Nørskov J K 1999 *Phys. Rev. B* **59** 7413
- [12] Noggle J H 1985 *Physical Chemistry* (Boston: Little, Brown and Co.)
- [13] Goodman D W, Kelley R D, Madey T E and Yates J T Jr 1980 *J. Catal.* **63** 226
- [14] Vannice M A 1976 *J. Catal.* **44** 152
- [15] Nielsen A (ed) 1995 *Ammonia: Catalysis and Manufacture* (Berlin: Springer)
- [16] Bligaard T, Nørskov J K, Dahl S, Matthiesen J, Christensen C H and Sehested J 2004 *J. Catal.* **224** 206
- [17] Andersson M P, Bligaard T, Kustov A, Larsen K E, Greeley J, Johannessen T, Christensen C H and Nørskov J K 2006 *J. Catal.* **239** 501
- [18] Nørskov J K, Bligaard T, Logadottir A, Bahn S, Hansen L B, Bollinger M, Bengaard H, Hammer B, Sljivancanin Z, Mavrikakis M, Xu Y, Dahl S and Jacobsen C J H 2002 *J. Catal.* **209** 275
- [19] Honkala K, Hellman A, Remediakis I N, Logadottir A, Carlsson A, Dahl S, Christensen C H and Nørskov J K 2005 *Science* **307** 555
- [20] Bligaard T, Honkala K, Logadottir A, Nørskov J K, Dahl S and Jacobsen C J H 2003 *J. Phys. Chem. B* **107** 9325
- [21] Pallassana V and Neurock M 2000 *J. Catal.* **191** 301
- [22] Liu Z-P and Hu P 2001 *J. Chem. Phys.* **114** 8244
- [23] Alcalá R, Mavrikakis M and Dumesic J A 2003 *J. Catal.* **218** 178
- [24] Ozaki A and Aika K 1981 *Catal. Sci. Technol.* **1** 87
- [25] Jacobsen C J H, Dahl S, Clausen B S, Bahn S, Logadottir A and Nørskov J K 2001 *J. Am. Chem. Soc.* **123** 8404